

Spatial organization of inhibitory synapses on dendritic arbor modifies activity patterns in a model of V1

Maggie Henderson
Dept. of Neurosciences
U.C. San Diego
La Jolla, CA 92093
mmhender@ucsd.edu

Bethanny Danskin
Dept. of Neurosciences
U.C. San Diego
La Jolla, CA 92093
bdanskin@ucsd.edu

Abstract

Recent work has suggested that dendrites act as a key organization unit of pyramidal neurons, integrating local inputs to generate complex neural response properties. In computational models of cortical networks, incorporating the integrative properties of dendrites, for instance by directing the landing of synapses to particular compartments on the dendritic arbor, and can increase the accuracy of a model at describing the input-output functions of realistic neurons. In this study, we sought to determine how the concentration of local inhibitory synapses on either the proximal or distal portion of dendrites of primary visual cortex neurons would modify the gain of the network. We used a model of exponential integrate and fire neurons to simulate the network, and found that landing of inhibitory synapses on the proximal portion of the dendrite resulted in an increased network gain relative to distal landing. These observations suggest that the spatial patterning of synapses is an essential component in generating cortical models that accurately capture biological data.

1 Introduction/Background

1.1 Computational role of dendrites in neural network models

Computational models of neural networks are a useful way to gain insight into the properties of biological neural networks. An advantage of using simulations is that they can be used to construct and observe large-scale networks of neurons, but generally require less time and expense than experimental techniques such as electrophysiology. However, one limitation of using computational simulations to study neural networks is that the models often must make simplifying assumptions about the properties of biological neurons. Simplifications can often increase the computational efficiency of a neural networks model, but may limit its biological applicability.

In models of cortical regions such as visual cortex, a common simplifying assumption is the reduction of each cortical pyramidal neuron to a single compartment. In models of this kind, each neuron is treated as a point-like node, and the output of a neuron is modeled as either a linear, nonlinear, or thresholded function of its summed inputs (Vanni et al., 2015). However, recent work has suggested that the transfer functions of real neurons are more accurately described by complex functions related to the structure of neurons, particularly its dendritic morphology. For instance, the efficacy of synaptic transmission to a neocortical pyramidal neuron is partially determined by where it lands on the dendritic tree (Williams & Stuart,

2002). Furthermore, evidence suggests that dendritic compartments can act as independent units for signaling and processing, and may serve as the basic units for integrating synaptic input (Branco & Hauser, 2010). These observations suggest that the applicability of cortical network models can be significantly improved by the incorporation of dendritic compartments with biophysically accurate properties.

1.2 Anisotropic landing in a model of visual cortex

A recent paper from Heikkinen and colleagues demonstrated the explanatory power of a model that incorporates dendritic computations (Heikkinen et al., 2015). This group used compartmental neurons to generate a model of primary visual cortex, and manipulated the spatial position of synaptic landings on the dendritic compartments of neurons. Under a variety of synaptic configurations, they simulated activity in the network in response to a visual stimulus, and recorded both the synaptic conductance and spiking output of neurons, in order to measure, respectively, the input and output tuning functions of the neurons. It was found that when feedback from extrastriate visual cortex was concentrated on the distal branches of dendrites, the input and output functions of model V1 neurons could be effectively separated, and were close to those predicted from empirical data. This result suggests that the anisotropic landing of feedback synapses on V1 neurons can have a significant effect on neural tuning, and raises the question of how other manipulations of synaptic connectivity in this network might modulate its output properties. Specifically, it has not been conclusively determined how the landing of local inhibitory synapses might modify the output of this network.

1.3 Goals/outcomes of this study

The goal of this study was to examine how anisotropic landing of local inhibitory synapses on the apical dendrites of model neurons affects the response properties of primary visual cortex. To achieve this, we generated a model of primary visual cortex, intended to capture the computational properties of the compartmental model described above (Heikkinen et al., 2015). Using exponential integrate and fire neurons, we were able to generate realistic patterns of spiking behavior. We also examined the response properties of individual compartmental neurons, and recovered several key observations from electrophysiology. We then manipulated the landing of inhibitory synapses on V1 pyramidal neurons and examined the output of the network. It was found that concentration of inhibition in the proximal dendrites resulted in lower mean activity with an increased signal to noise ratio (SNR), while inhibition in the distal dendrites resulted in greater mean activity with a lower SNR.

2 BRIAN neuron simulator

To implement our model we used the neuron simulator platform BRIAN (Goodman and Brette, 2008), using both built-in functionality and additions.

Code for the model is made available with this manuscript

3 Exponential integrate and fire model

The exponential integrate and fire (EIF) neuron model approximates neural behavior by reducing the dynamic system to a single differential equation. This makes it less computationally intensive to model many neurons at once.

3.1 EIF neuron simulation

There are three components to the simulated neuron's behavior. The first is passive RC neuron behavior around the resting membrane potential V_L .

The second is exponential behavior around the threshold potential V_T , where the neuron will

entire a regime where the membrane potential rapidly increases to infinity. For the purposes of modeling a neuron's behavior, at some cut-off potential $V_{Cut-off}$ the membrane potential is reset to near the resting potential, a value known as V_{Reset} , and the behavior continues.

The third component is the summation and integration of the synaptic inputs, in the form of multiple currents $I_{dendrites}$. The equation for the EIF model is:

$$C \frac{dV}{dt} = g_L(V_L - V) + \varphi(V) + \sum I_{dendrites}(t)$$

$$\varphi(V) = g_L \Delta T e^{V - V_T / \Delta T}$$

where $\varphi(V)$ is the nonlinear spiking current near threshold, ΔT is the spike slope factor, C the membrane capacitance and g_L the leak conductance

99

3.1.1 Parameters of the EIF neuron

The parameters for the V1 excitatory pyramidal cells, as taken from Heikkinen et al. 2015, are as follows:

103

Table 1: V1 EIF paramters

104

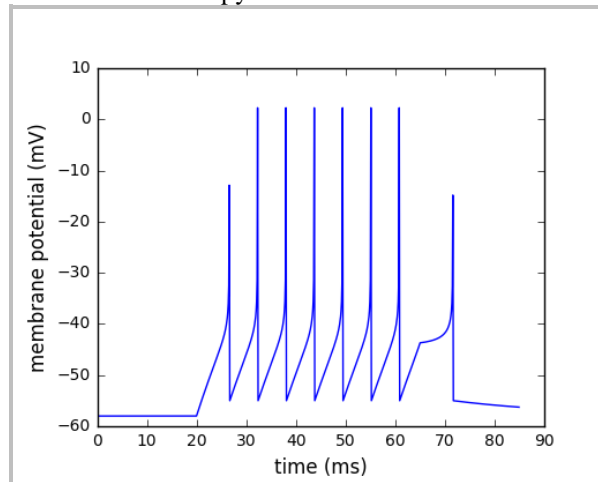
Passive Properties		
C	200 pF	Membrane capacitance
g_L	8.4 nS	Leak conductance
E_L	-58 mV	Leak (rest) potential
EIF properties		
V_T	-38 mV	Threshold potential
V_R	-55 mV	Reset potential
ΔT	2 mV	Threshold slope factor
V_{cut}	-20	Cut-off voltage for action potential
Differential equation		
$dv/dt = (g_L * (E_L - v) + g_L * \Delta T * \exp((v - V_T) / \Delta T) + I) / C$		

105

3.2 EIF single neuron behavior

A single EIF neuron with a constant current injection shows spiking behavior, with return to rest. All parameters taken from the V1 pyramidal cells as outline above.

108



109

Figure 1: Single EIF neuron with 0.6 nA of injected current.

110

111 Near to threshold there is unstable behavior, as illustrated by the final spike after the injected
112 current has ended. Because the membrane potential is in the exponential regime the potential
113 does not return to baseline and instead eventually fires a delayed spike.

114 **3.3 EIF neuron network**

115 To examine the behavior of an EIF neuron in a network, we set up a simple test, with 25
116 input neurons synapsing onto the soma, with a mixture of both excitatory and inhibitory
117 synapses. The parameters for such synapses are:

118 **Table 2: V1 EIF synaptic parameters**

119

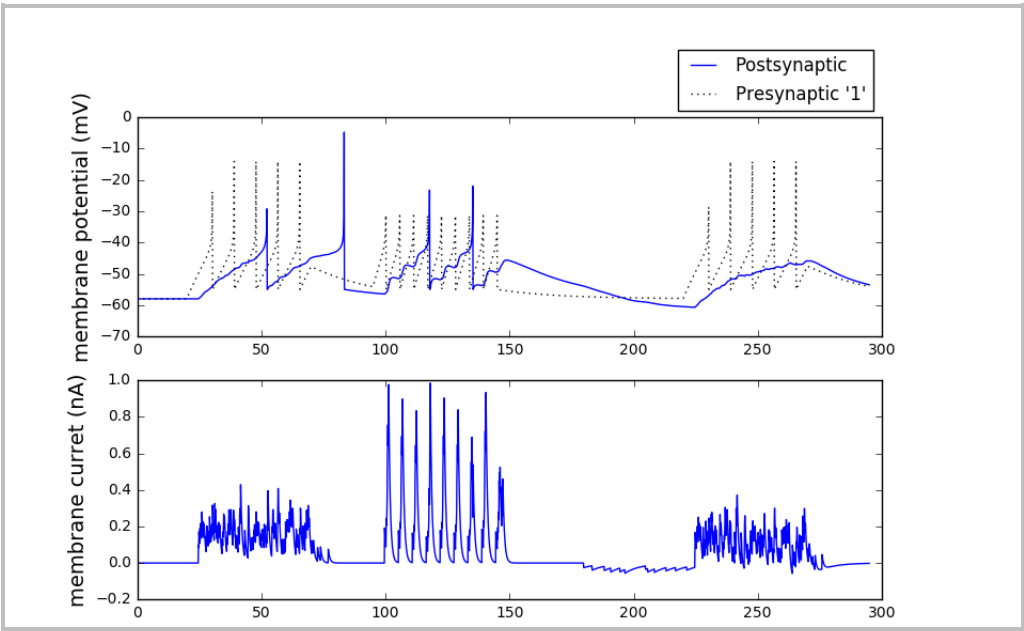
Synaptic parameters		
E_{AMPA}	0 mV	Reversal potential of the AMPA currents
T_{AMPA}	0.7 ms	Time constant of G_{AMPA} decay
G_{AMPA}	1.7 nS	Peak conductance for AMPA synapse
E_{GABA}	-75 mV	Reversal potential of the GABA currents
T_{GABA}	7 ms	Time constant of G_{GABA} decay
G_{GABA}	1.2 nS	Peak conductance for GABA synapse

120

121 The behavior of the network is as illustrated in the figure. With many excitatory inputs the
122 post-synaptic EIF neuron integrates the depolarizations until approaching threshold. After
123 spiking the EIF neuron resumes integrating the inputs. If the input neurons are correlated in
124 their spike timing the EIF neurons summates appropriately and may spike more than if the
125 individual inputs were random and had thus decayed.

126 The addition of a small number of inhibitory cells to the network is sufficient to suppress
127 spiking to the same inputs that previously evoked spiking.

128



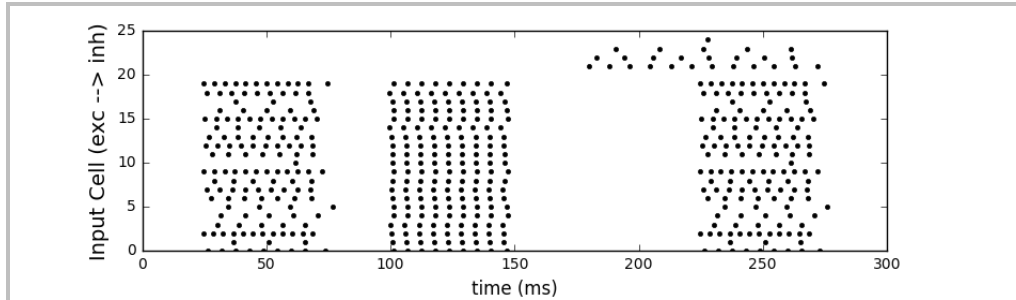


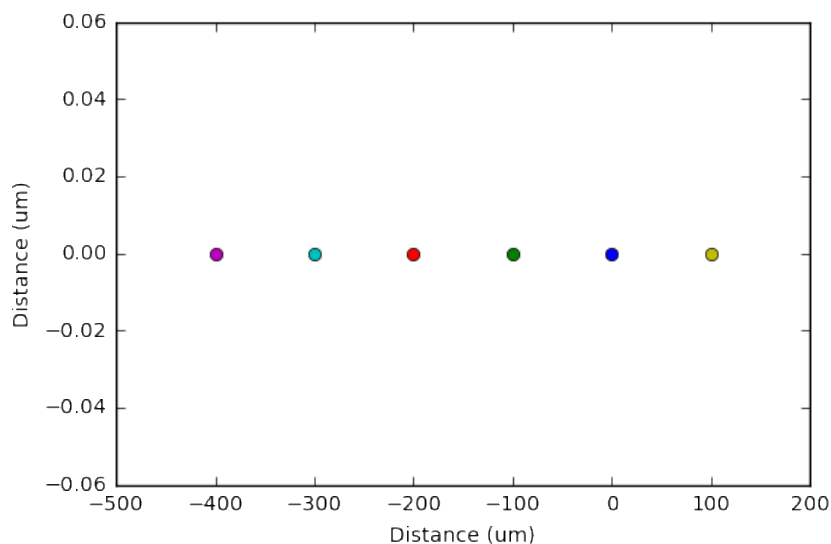
Figure 2: EIF neuron network. Top: the spiking behavior of the post-synaptic EIF neuron and an example input neuron. Middle: record of the synaptic currents underlying the membrane potential. Bottom: spike raster of the input neurons, each receiving a different injected current, those making both excitatory and inhibitory synapses.

4 Spatial neuron

In order to directly examine the integrative properties of dendrites in pyramidal neurons, we used the BRIAN neural simulator to construct spatial neurons having six compartments. In keeping with the methods of Heikkinen and colleagues, we used four apical compartments, one basal compartment, and one somal compartment. We used a somal diameter of 30 microns, and total lengths of 100 and 400 microns for the basal and apical dendrites, respectively.

4.1 Passive decay of EPSPs

To examine the passive conductance properties of this compartmental model, we stimulated the neuron with synaptic input to generate EPSPs. We directed this synaptic input to one compartment at a time, and examined the voltage time course of the EPSP in the soma. As shown in Figure 3, we found that when the synaptic input was directed to the soma, EPSP amplitude was largest. As the site of synaptic input moved further from the soma, either to the apical or basal dendritic compartment, the EPSPs were similar in shape but lower in amplitude. The decay in amplitude with distance was roughly exponential. This attenuation in EPSP amplitude with distance from the soma is an accordance with experimental observations from cortical pyramidal neurons (Williams & Stuart, 2002).



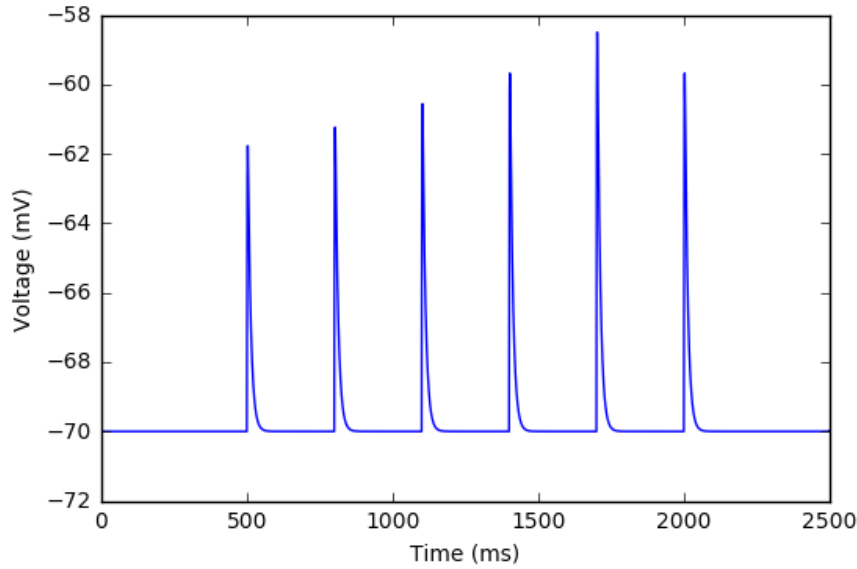


Figure 3. Top: The location of each of the 6 compartments in an example spatial neuron, with soma at $x=0$. Bottom: Synaptic activity was used to generate EPSPs. A synaptic input was directed to one compartment of the neuron at a time, moving from left to right along the neuron, and voltage was recorded at the soma.

4.1 Modeling the passive decay of EPSPs

The above observations support an exponential function for the decay of EPSP amplitude with distance from the soma. In order to model this decay, we calculated a space constant for the spatial neuron described above. We then calculated the amount of attenuation predicted for synaptic inputs on the distal, proximal, and somatic compartments according to the following equation:

$$a = e^{-x/\tau}$$

Where x is the distance of the input from the soma, and τ is the space constant ($\tau = 0.629$ mm). This gave a multiplier for each compartment:

Table 3: Spatial neuron parameters

	Soma	Proximal	Distal
x	0 μm	100 μm	400 μm
a	1	0.85	0.53

Then, when building our network, we used these multipliers to scale the effect of each synaptic event, depending on which compartment the synapse was directed to.

5 Constructing a model of visual cortex

5.1 Anatomical connections of visual cortex

Primary visual cortex (V1) is composed of several feedback and feedforward circuits that form the classical representation of visual space. Each layer maintains a topography, and has

connections to and from areas with similar topography.

Visual information enters V1 from the LGN in feedforward projections to excitatory pyramidal cells. These excitatory neurons in V1 send feedforward projections to extrastriate pyramidal cells, and collaterals to local V1 excitatory and inhibitory cells.

The extrastriate neurons send feedback projections to V1, and inhibitory interneurons in V1 also feedback onto the pyramidal cells. The specificity of these projections, and the relative spatial spread of connections has been detailed in anatomical studies (Nauhaus et al., 2008)

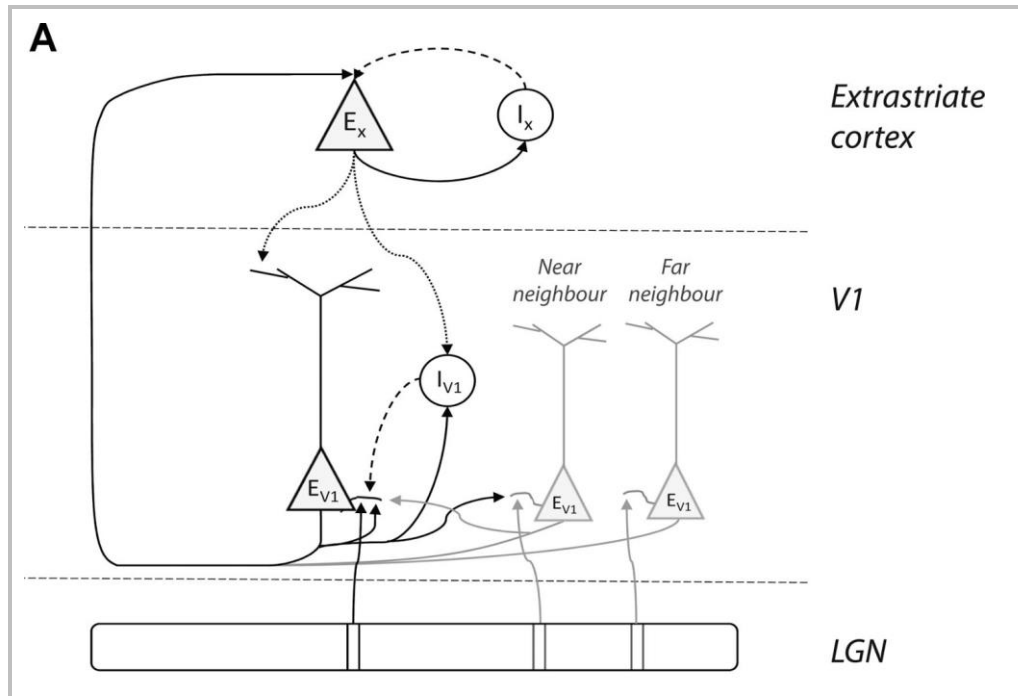


Figure 4: Schematic of visual cortex network. Taken from Heikkinen et al., 2015.

Our model incorporates a single-layered V1 with LGN feedforward neurons, reciprocal excitation to extrastriate feedback neurons, and local reciprocal excitation and inhibition.

Due to computational constraints, we modeled the connections of V1 with only a fraction of the neurons modeled in Heikkinen et al. 2015. There are 400 V1 excitatory neurons, 400 LGN neurons, 100 extrastriate neurons, and 100 V1 inhibitory neurons

5.2 Lateral inhibition in the model

The lateral inhibition from local GABAergic inhibitory neurons is modeled as having a spatial extent of about 1 mm. However, to produce the center-surround suppression of activity seen in cortex, we introduced a lack of inhibitory connections for completely overlapped spatial populations, as schematized in the following connection diagram

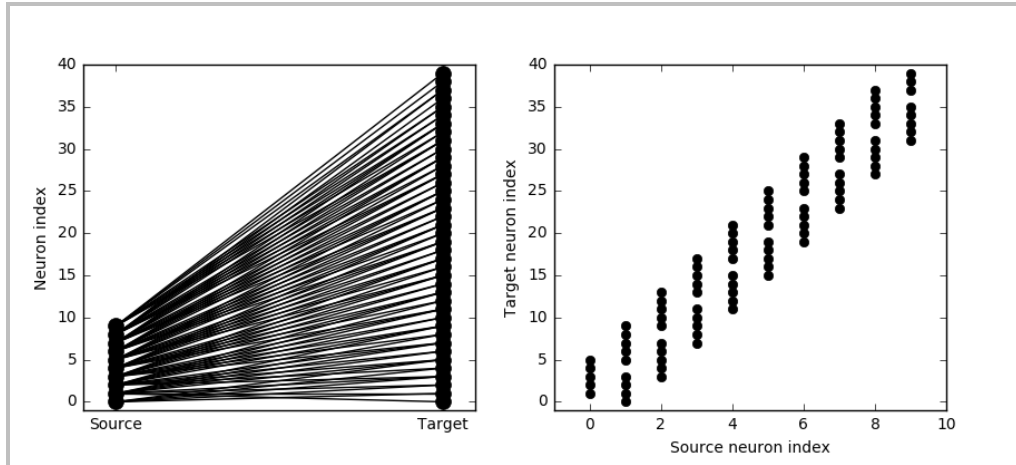


Figure 5: Schematic of local inhibitory synaptic connections in V1

5.3 Extrastriate Feedback connections in the model

The extrastriate feedback connections have greater spatial spread than the feedforward connection from LGN to V1 (roughly 1:1), feedforward from V1 to extrastriate (convergence, 4:1) or the lateral excitation and inhibition of V1. The extrastriate excitation has a broad spatial extent, as schematized by the diverging connections and large number of synapses.

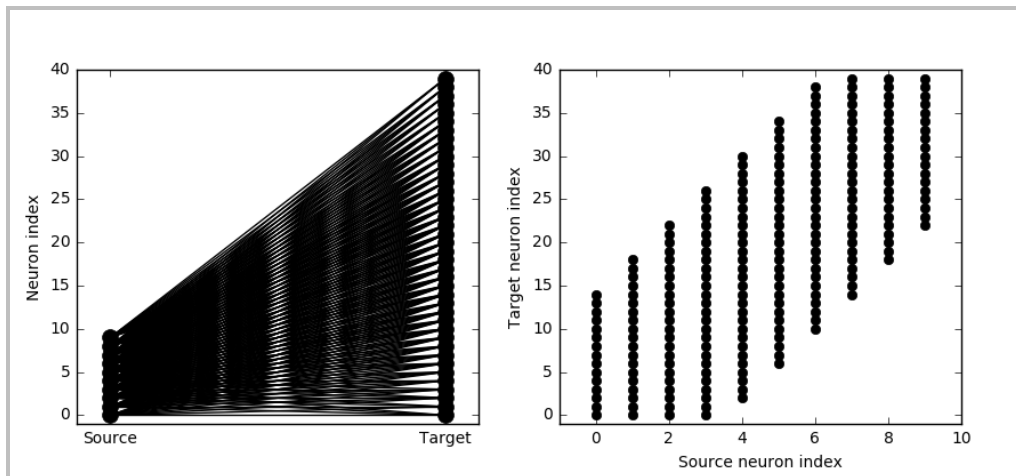


Figure 6: Schematic of extrastriate feedback connections in V1

6 Impact of the synapse location on network behavior

The innovation of this model is the ability to change the effective location of the synapses, as well as the convergence and divergence of network nodes. Thus we can model how the network behaves if the synapses land on different locations in the dendrites. Specifically, changing from a proximal dendrite to a distal dendrite can change the integration in the circuit.

As described in Section 4.1, we modeled the effect of synapses on different compartments by computing the space constant of the exponential decay of EPSP amplitude with distance from the soma. Therefore, synapses on more distal regions of the dendrite would have a lower efficacy than synapses on more proximal regions.

6.1 Location of inhibitory synapses changes network gain

Moving the site of local inhibition from a proximal dendrite to a distal dendrite reduces the absolute effect of inhibition in the circuit.

For example, if the circuit is fed a random background of activity from LGN inputs, except for a correlated area of activity (spatial extent ~5 mm) across 30 LGN neurons, the activity throughout the circuit reflects this input. Specifically, there is broad spiking activity throughout V1 and extrastriate neurons, while peak spiking occurs amongst the downstream neurons with the same spatial position as the 30 LGN neurons.

If the inhibitory synapses are on the proximal dendrite, the effect of inhibition on the network is stronger, and thus network activity as a whole is reduced (mean spike rate: 14.7 Hz proximal; 17.4 Hz distal). However, the signal to noise ratio is improved due to the reduced network gain (SNR 3.39 with proximal input). If the synapses are on the distal dendrites, network activity, including the uncorrelated activity, is greater. Therefore there a lower SNR (3.14 with distal input).

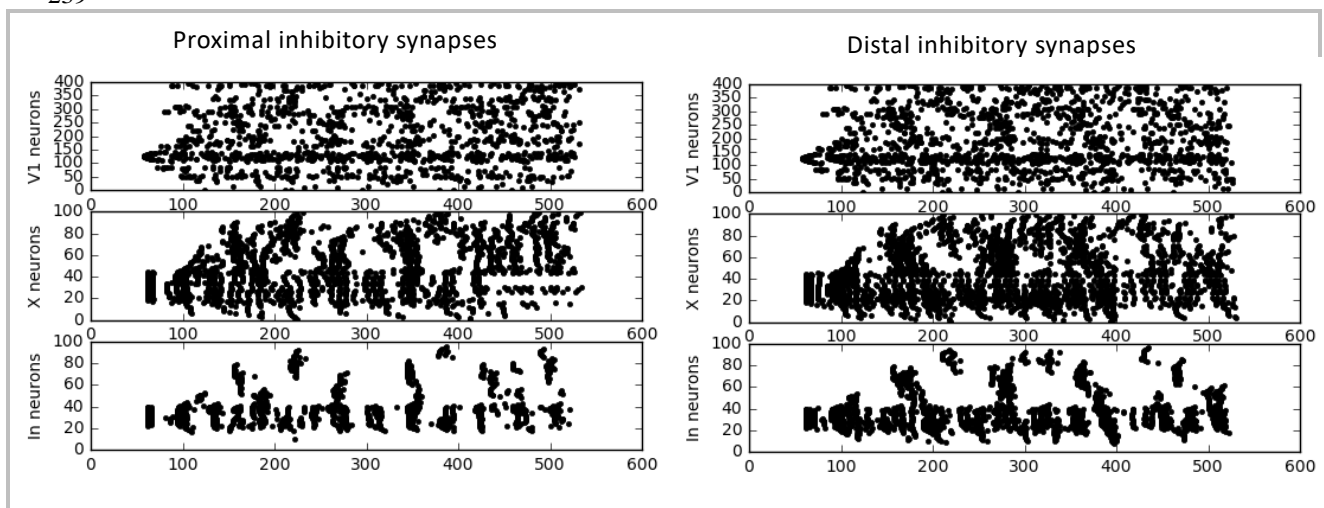


Figure 7: Effect of distal vs. proximal inhibitory synapses on network gain. Top: spike raster of the V1 excitatory neurons. Middle: spike raster of the extrastriate excitatory neurons. Bottom: spike raster of the local V1 inhibitory neurons. Correlated LGN input occurs amongst V1 neurons 100-130.

7 Discussion and Future Directions

As described above, we demonstrated that manipulating the spatial organization of local inhibitory synapses on the apical dendrites of pyramidal neurons in a model of V1 modified the gain of the network response. Specifically, concentration of synapses at the proximal region of dendrites resulted in lower overall activity, accompanied by a higher SNR, while concentration of synapses at the distal region resulted in a lower SNR. Computationally, this suggests that the role of local inhibitory synapses may differ depending on how close to the soma they land. For instance, local inhibition to the proximal portion of the apical dendrite may be used to limit the spread of cortical responses, by suppressing responses in neurons that are only weakly excited. Conversely, local inhibition to the distal portion results in less suppression overall, which could be useful for generating large, nonspecific responses to stimuli.

There are several aspects of this model which could be improved and/or extended in future implementations. One limitation is that we did not explore the interactions between multiple synapses on a particular portion of the dendrite. For instance, the response to multiple simultaneous synaptic inputs is often not a linear sum of the responses to the inputs alone,

261 and it would be interesting to investigate how nonlinearities in the responses to multiple
262 inputs could impact the integrative properties of this model. Another potential way to extend
263 this model would be to place synapses at intermediate distances along the dendrite, and look
264 at how the response properties differ when synapses are directed to an intermediate distance
265 rather than the most proximal or distal compartment. Finally, it would be informative to
266 examine how synapse configuration the response properties the other neurons in the model.
267 For instance, we could examine the gain of responses in extrastriate neurons for proximal
268 versus distal landing of synapses from V1.

269 Furthermore, it would be interesting to adapt this model for other cortical regions, such as
270 motor cortex or prefrontal cortex. It is likely that some of the same principles would apply,
271 however, introducing inputs and outputs from a larger range of cortical regions could
272 introduce new patterns of dendritic integration. Future work will be necessary to determine
273 how synapse landing configurations can modify the behavior of more complex networks.

274

275 **References**

- 276 Branco, T., & Häusser, M. (2010). The single dendritic branch as a fundamental functional unit in the
277 nervous system. *Current Opinion in Neurobiology*, 20(4), 494–502.
- 278 Goodman DF and Brette R (2009). The Brian simulator. *Front Neurosci*
279 doi:10.3389/neuro.01.026.2009
- 280 Heikkinen H, Sharifian F, Vigario R, Vanni S. Feedback to distal dendrites links fMRI signals to
281 neural receptive fields in a spiking network model of the visual cortex. *J Neurophysiol*. Jul;114(1):57-
282 69, 2015.
- 283 Nauhaus I, Busse L, Carandini M, Ringach DL. Stimulus contrast modulates functional connectivity in
284 visual cortex. *Nat Neurosci* 12(1):70-6, 2009
- 285 Vanni, S., Sharifian, F., Heikkinen, H., & Vigário, R. (2015). Modeling fMRI signals can provide
286 insights into neural processing in the cerebral cortex. *Journal of Neurophysiology*, 114(2).
- 287 Williams, S. R., & Stuart, G. J. (2002). Dependence of EPSP Efficacy on Synapse Location in
288 Neocortical Pyramidal Neurons. *Science*, 295(5561), 1907–1910.